Available online at www.CivileJournal.org

Civil Engineering Journal

(E-ISSN: 2476-3055; ISSN: 2676-6957)

Vol. 11, No. 07, July, 2025

LiDAR-Based Pothole Patching Quantity Estimation and Cost Saving Analysis Using Segmented TIN Model

N. H. Riyaz Khan [1], S. Vasantha Kumar [1*]

[1] *School of Civil Engineering, Vellore Institute of Technology (VIT), Vellore, 632014, Tamil Nadu, India.*

Received 05 March 2025; Revised 17 June 2025; Accepted 22 June 2025; Published 01 July 2025

Abstract

Potholes represent a significant form of road distress, and the conventional method for estimating the required repair material typically assumes a cuboidal shape for each pothole. This approximation often leads to an overestimation of pothole volume, resulting in excessive patching material and increased costs. To address this limitation, the present study introduces a LiDAR-based segmentation and digitization method. This approach utilizes only the point cloud data of potholes obtained via terrestrial laser scanning to generate accurate 3D surfaces, contours, and a Triangulated Irregular Network (TIN), thereby enabling precise volume and patching quantity calculations. The findings revealed that the volume and patching quantity estimated using the traditional cuboidal method are two to four times greater than those calculated through the proposed LiDAR-based approach. This clearly demonstrates that the conventional method leads to unnecessary procurement of patching materials. Cost analysis further indicated that the LiDAR-based approach could result in savings of approximately INR 3,500 per pothole in India, $262 in the USA, and £150 in the UK. Given that millions of potholes are repaired annually in each country, adopting the proposed LiDAR-based method has the potential to yield substantial cost savings on a national scale.

Keywords: Potholes; Terrestrial LiDAR; Contours; Triangulated Irregular Networks; Volume; Patching Quantity.

1. Introduction

Roads play a vital role in the development of any nation, serving as an essential component of a country's infrastructure. In India, the highway sector has received the highest allocation in the Union Budget in recent years, reflecting the government's ambitious plans to expand the national highway network from the current 146,000 km to 200,000 km by 2037, and access-controlled expressways from 4,000 km to 50,000 km within the same timeframe [1]. This clearly underscores the strategic importance of the road and highway sector, which not only attracts global investment but is also critical to sustaining the country's economic growth. However, simply expanding the road network is not enough. A key factor in ensuring the long-term effectiveness of these infrastructure developments is the quality of maintenance. Proper road maintenance requires regular evaluation of pavement conditions, as riding quality and structural integrity naturally deteriorate over time due to traffic loads and environmental factors [2, 3]. When pavements fall into poor condition, it leads to higher vehicle operating costs and increased delays for road users. Therefore, it is essential to conduct periodic pavement assessments to guide maintenance interventions and ensure roads remain in acceptable condition.

A core component of road maintenance is the Pavement Management System (PMS), which involves evaluating pavement roughness, surface distress, and skid resistance. Among these parameters, surface distresses are considered

* Corresponding author: svasanthakumar@vit.ac.in

http://dx.doi.org/10.28991/CEJ-2025-011-07-021

the most critical, as they directly impact road safety. Potholes are among the most common and recognizable forms of pavement distress encountered by road users. These bowl-shaped depressions in the asphalt surface typically form under the stress of heavy traffic during the winter or rainy seasons. The deterioration process is accelerated by water infiltration through fatigue-induced alligator cracking or low-temperature cracking, which weakens the pavement structure. Eventually, this leads to the erosion of the base or subgrade and the formation of potholes. The presence of potholes on road surfaces contributes to various negative outcomes, including accidents, traffic congestion, and decreased vehicle fuel efficiency. Compared to other distresses such as rutting and ravelling, potholes pose a greater hazard. In fact, potholes were responsible for 4,450 road accidents and 1,900 fatalities in a single year—equivalent to nearly five deaths per day in India [4]. Alarmingly, pothole-related accidents are on the rise, with a 22.6% increase reported over the previous year. These statistics clearly highlight the urgent need for regular pothole maintenance and repair, particularly in developing countries like India, where road safety remains a critical concern.

Highway agencies typically employ a rehabilitation technique known as patching, in which a suitable material—either hot or cold mix asphalt—is placed into the pothole after removing debris and is then compacted to prevent future deterioration. Pothole repair methods generally fall into three categories: Throw-and-Go, Throw-and-Roll, and Semi-Permanent. In the Throw-and-Go method, the patching material is simply poured into the unprepared pothole until it is filled. While this method is simple, labor-efficient, time-saving, and cost-effective, its durability is questionable, as the uncleaned pothole may still contain debris and water, and the lack of compaction can lead to premature failure. A step above this is the Throw-and-Roll method, where compaction is performed using the tires of a truck. This offers slightly better performance due to some degree of compaction, though it still lacks the thorough preparation found in more permanent repairs. The Semi-Permanent approach is considered the most effective of the three. It involves first removing debris and water from the pothole, followed by the application of a tack coat. The patching material is then placed and compacted thoroughly using vibratory rollers. Due to the improved preparation and compaction, this method offers significantly better durability and longevity compared to the previous two. While each method has its own set of advantages and limitations, the choice of technique typically depends on the total patching cost, which includes labor, equipment, and material expenses. Accurate estimation of the required quantity of patching material is essential. Underestimating the amount can lead to incomplete filling and inadequate compaction, whereas overestimation results in unnecessary transportation costs and material waste.

The current method for estimating the quantity of patching material relies on calculating pothole volume based on simple geometric measurements—length, width, and depth [5–7]. However, this approach lacks accuracy, as potholes are typically irregular in shape rather than rectangular. Consequently, volume estimates based on these dimensions may not reflect the true volume, leading to inaccurate material estimation. To address this limitation, recent studies have turned to the use of 3D modeling techniques for more precise volume estimation. Technologies such as digital photogrammetry (using stereo images) [8, 9] and Mobile Light Detection and Ranging (LiDAR) [10, 11] have been increasingly adopted. However, stereo imagery is highly sensitive to lighting conditions, shadows, and low contrast between the pothole and surrounding pavement, all of which can significantly affect detection accuracy and the quality of the resulting 3D model [12].

Another challenge with image-based approaches is the need for large datasets to train detection models. For instance, Ruseruka et al. (2024) [13] trained their YOLO model using 1,876 pothole images captured via dashboard-mounted smartphones. Similarly, Park & Nguyen (2025) [14] used a dataset of 1,890 pothole images from Korea for their YOLOv8 model, while Zhong et al. (2025) [15] employed 5,000 high-resolution pothole images from China. Given that deep learning models like YOLO require vast training datasets, researchers have increasingly turned to mobile LiDAR systems for more accurate and efficient pothole detection and measurement [10, 11]. For example, Faisal and Gargoum (2025) [16] utilized the Leica Pegasus TRK 700 NEO mobile LiDAR system to capture pothole data along a 2.7 km road in Alberta, Canada. Talha et al. (2024) [11] applied the Ouster OS0 mobile LiDAR system in conjunction with a Global Navigation Satellite System (GNSS) for detecting potholes on a section of Interstate 71 in the United States. Despite their effectiveness, mobile LiDAR systems present major challenges, including high costs—professional-grade systems can exceed $300,000—alongside the need for skilled operators and substantial data storage capabilities in the terabyte range [17, 18].

It is important to note that in most existing studies, even when 3D models are generated using close-range photogrammetry or mobile LiDAR, the volume of potholes is still often estimated using basic length, width, and depth measurements. As previously mentioned, this cuboidal assumption does not accurately reflect the irregular shape of real potholes, potentially leading to overestimation of volume and unnecessary use of repair material. Moreover, there has been little to no focus in the literature on quantifying the material savings that could result from using accurate 3D models. Such an analysis is crucial, as adopting precise 3D volume calculations could significantly reduce asphalt usage compared to traditional rectangular-based assumptions.

To address the limitations identified in existing studies—such as the need for large datasets, the high cost of mobile LiDAR systems, reliance on basic length/width/depth measurements, and the lack of research on patching quantity estimation and cost comparison—the present study proposes a novel approach utilizing Terrestrial (ground-based) LiDAR for generating 3D models of potholes and accurately estimating the required patching material. Unlike deep

learning models that demand extensive training data, the proposed method requires only the point cloud data of the specific pothole under investigation, which is sufficient for precise volume estimation through segmentation and digitization.

This approach employs only terrestrial LiDAR, which is significantly more affordable than mobile LiDAR systems. For instance, the Leica imaging terrestrial laser scanner used in this study costs approximately $30,000—just one-tenth the cost of a typical mobile LiDAR setup. In contrast to traditional methods that estimate pothole volume using simplified rectangular assumptions (length × width × depth), the proposed method extracts the actual pothole boundaries through segmentation, allowing for highly accurate volume and material quantity estimation. In addition to addressing key gaps in the existing literature, the proposed approach offers several practical advantages. The specific objectives of this study are as follows:

- To scan selected potholes of varying sizes and shapes on urban and rural roads using Terrestrial LiDAR and to post-process the registered scans for noise and outlier removal.
- To segment the pothole-affected regions using profile graphs and digitize the exact boundaries in a GIS environment to isolate the pothole's point cloud.
- To generate contours, 3D surfaces, and Triangulated Irregular Network (TIN) models to calculate accurate pothole volumes and the required patching material.
- To compare the estimated patching quantities derived from the proposed Terrestrial LiDAR-based approach with those obtained using the conventional rectangular volume method, highlighting the potential cost savings.

The structure of this research article is organized as follows: The Introduction presents the significance of pavement maintenance, with a focus on potholes, and provides a comprehensive review of previous studies on pothole detection and geometry estimation. It also outlines the gaps identified in the literature and explains how this study addresses them, concluding with the objectives of the research. Section 2 describes the Materials and Methods, beginning with the study area (2.1) and LiDAR survey (2.2). The methodology is detailed in section 2.3 and divided into three subsections: Section 2.3.1 discusses the post-processing of LiDAR data and removal of noise and outliers. Section 2.3.2 elaborates on the segmentation of pothole-affected areas using cross-sectional plots and the digitization of pothole boundaries. Section 2.3.3 describes the generation of 3D surfaces, contours, and TINs to compute accurate pothole volumes and patching quantities, followed by a comparison with the conventional rectangular approach to demonstrate cost savings. Section 3 presents the results of the study, and Section 4 provides the concluding remarks.

2. Material and Methods

2.1. Study Area

The potholes for the present study were selected from typical urban and rural roads in and around the Katpadi town in Vellore city, which is located in the Tamil Nadu state of India. Figure 1 shows the location of the study area. A total of ten potholes were considered, as shown in Figure 2.

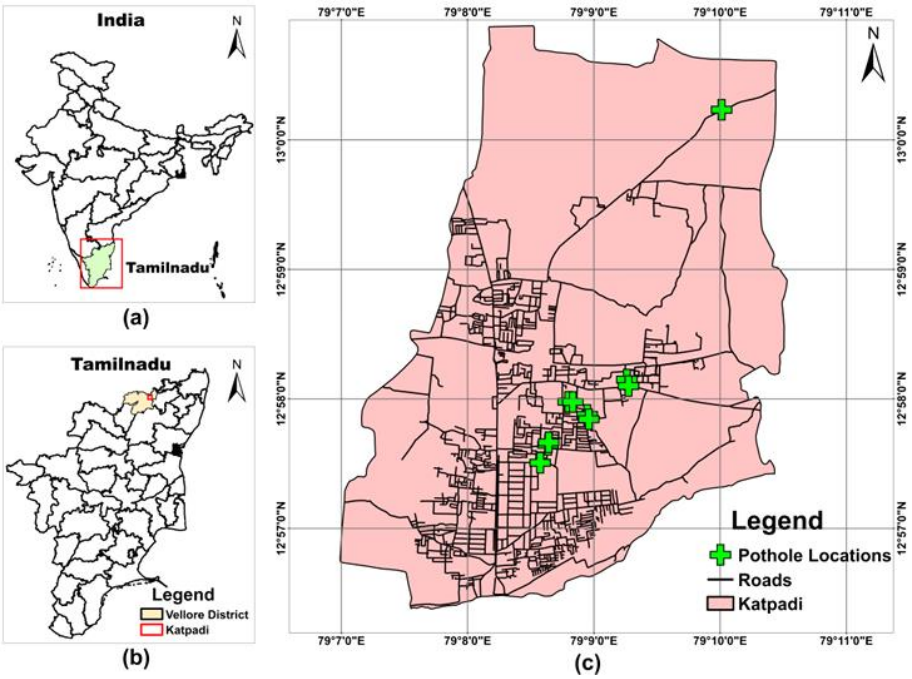

Figure 1. Map showing the location of (a) Tamilnadu state in India (b) Vellore district and Katpadi town in Tamilnadu state (c) Potholes considered in Katpadi town

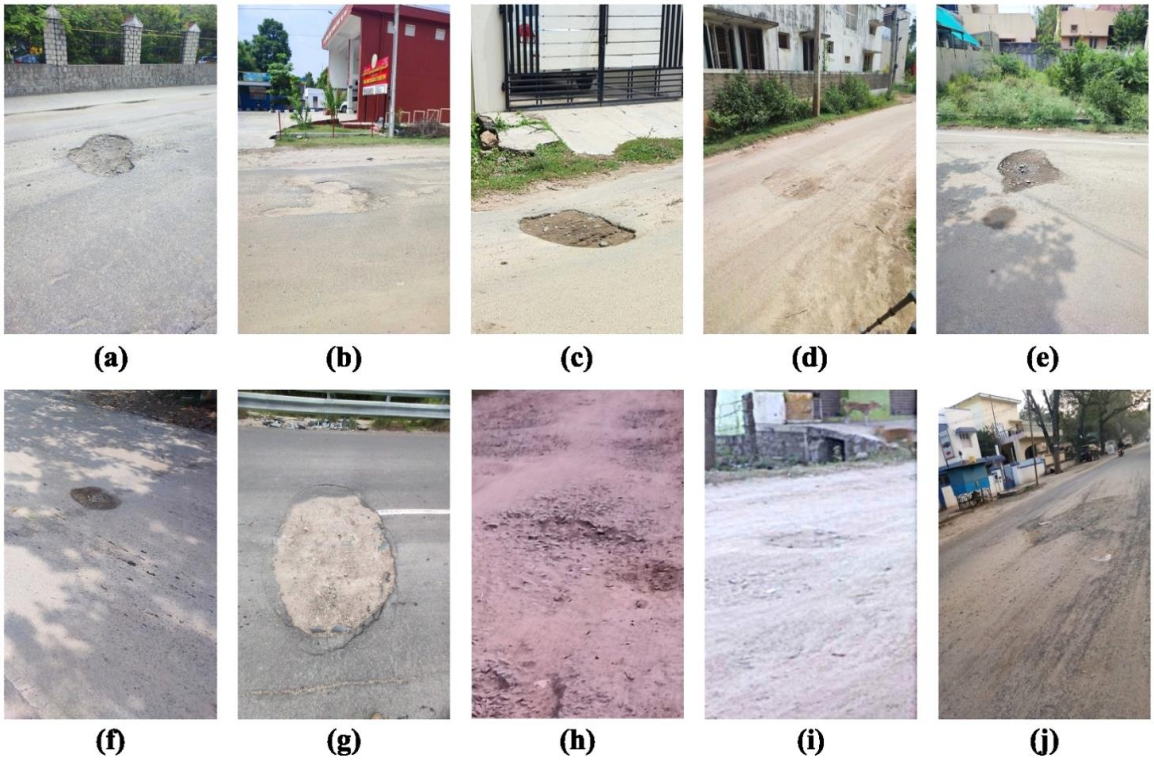

Figure 2. Potholes considered for the study

Potholes typically begin with the formation of cracks in the pavement, which, over time, lead to the disintegration of the asphalt mixture. If left untreated, these cracks gradually develop into bowl-shaped cavities that may extend down to the base course of the pavement. In this study, ten potholes were carefully selected to represent different stages of development. For instance, a pothole that has reached the base course is shown in Figure 2-a, while one confined to the surface course is illustrated in Figure 2-g. The selected potholes also vary in shape and size. As an example, the pothole in Figure 2-g has an oval shape, whereas Figure 2-c depicts a rectangular one. In general, most potholes observed on roads exhibit relatively standard shapes such as elliptical, circular, or oval, as seen in the images presented in Figure 2. However, some potholes do not conform to standard geometric forms and may take on irregular shapes. The current study also includes such cases—for example, the larger, unusually shaped potholes shown in Figures 2-b and 2-j. Thus, the ten potholes considered in this study encompass a range of shapes, sizes, and developmental stages. Consequently, they exhibit varying volumes and require different quantities of patching material. These differences can be accurately measured and analyzed using ground-based LiDAR surveying techniques, which are detailed in the following section.

2.2. Data Collection

The LiDAR scanning of potholes was conducted using the Leica imaging terrestrial laser scanner, a ground-based LiDAR instrument, as shown in Figure 3. The scanner is mounted on a tripod, allowing for easy deployment and operation. This study opted for ground-based LiDAR instead of aerial or UAV-based LiDAR due to several practical considerations. UAV LiDAR typically requires a licensed drone pilot, regulatory permissions, and skilled personnel, making it less convenient for localized pavement studies. Additionally, road environments—particularly those bordered by trees or overhead electrical cables—can obstruct UAV coverage.

In contrast, ground-based LiDAR offers a more accessible and efficient solution. The device can be positioned at ground level on the roadside, and with the push of a button, it performs a comprehensive scan of the pothole area. The laser scanner used in this study has a measurement speed of 360,000 points per second and a maximum range of 60 meters, meaning any object within that distance can be captured with high spatial resolution.

Scanning can be performed in standard or high-density modes, which determine the number of points generated in the point cloud. In standard mode, a typical scan takes about 2 minutes, while high-density mode requires approximately 4 minutes. Both modes were utilized in this study to assess whether standard density is sufficient for accurate pothole detection. As a result, higher point counts are observed in scans conducted in high-density mode (potholes ‘a’ to ‘f’ in Table 1), compared to those scanned in standard mode (potholes ‘g’ to ‘j’).

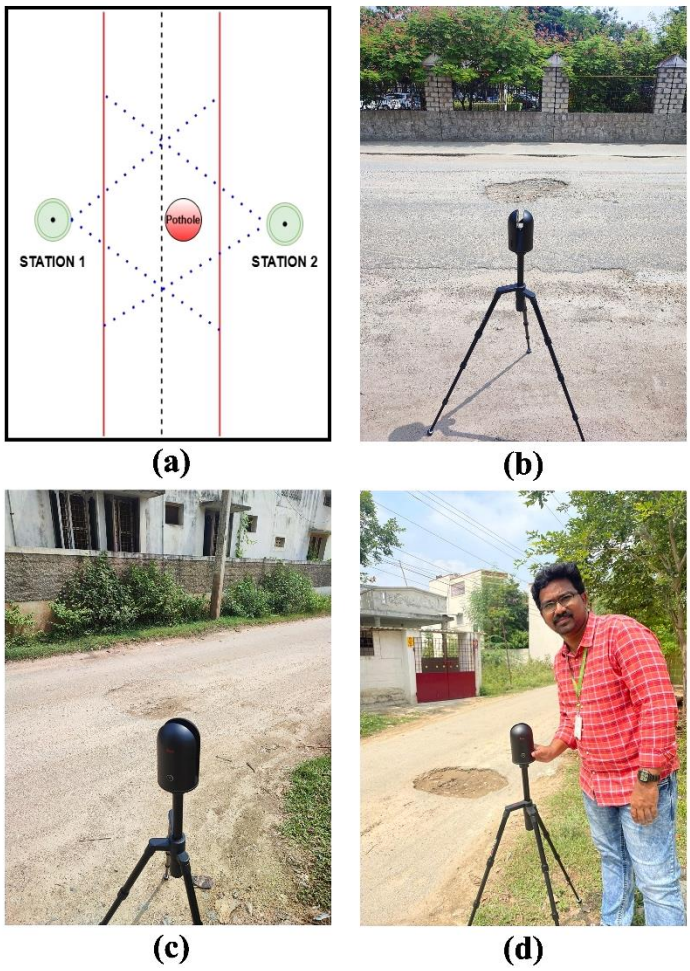

Figure 3. Sample photos taken during the data collection

Table 1. Point cloud details of the scanned potholes

S. No	Pothole ID	Point Count	Point Spacing (m)	No. of Scans
1	Pothole – 'a'	13,275,654	0.007	2
2	Pothole – 'b'	13,488,289	0.006	2
3	Pothole – 'c'	14,370,215	0.004	2
4	Pothole – 'd'	13,293,890	0.005	2
5	Pothole – 'e'	14,442,651	0.008	2
6	Pothole – 'f'		0.006	
7	Pothole – 'g'	4,582,551	0.039	1
8	Pothole – 'h'	8,604,700	0.033	1
9	Pothole – 'i'	7,872,804	0.016	1
10	Pothole – 'j'	8,722,635	0.032	1

Another reason for the higher point counts observed in potholes 'a' to 'f' is that each of these was scanned twice—once from each side of the road—using the setup illustrated in Figure 3-a. In contrast, potholes 'g' to 'j' were scanned only once, from the nearest side of the road. This setup allowed for an evaluation of whether two scans are necessary or if a single scan is sufficient to generate a 3D model of the pothole with the desired level of accuracy. The number of scans directly influenced the point spacing, as reflected in Table 1. For potholes 'a' to 'f', the average point spacing ranged between 4 mm and 8 mm, while for potholes 'g' to 'j', it ranged between 16 mm and 39 mm. This outcome is logically consistent: the more scans performed, the higher the point density, which results in smaller average point spacing due to the greater number of data points collected. Potholes 'e' and 'f' were located adjacent to each other and were thus captured within the same point cloud generated from the two scans conducted from both sides of the road. After the data collection was completed, the scans were imported into Leica Cyclone software for post-processing, the details of which are described in the Methodology section.

2.3. Methodology

The step-by-step methodology followed in this study is illustrated in the flowchart presented in Figure 4. The overall approach is divided into three main parts:

1. LiDAR data collection, post-processing, and noise removal;
2. Segmentation of the pothole-affected area based on cross-sectional plots and digitization of the pothole boundary;
3. Generation of 3D surfaces, contours, and a Triangulated Irregular Network (TIN) for accurately calculating the volume of the potholes and the required quantity of patching material, followed by a comparison with the conventional rectangular-based volume estimation to highlight potential cost savings in patching work.

Each of these steps is described in detail in the following sections.

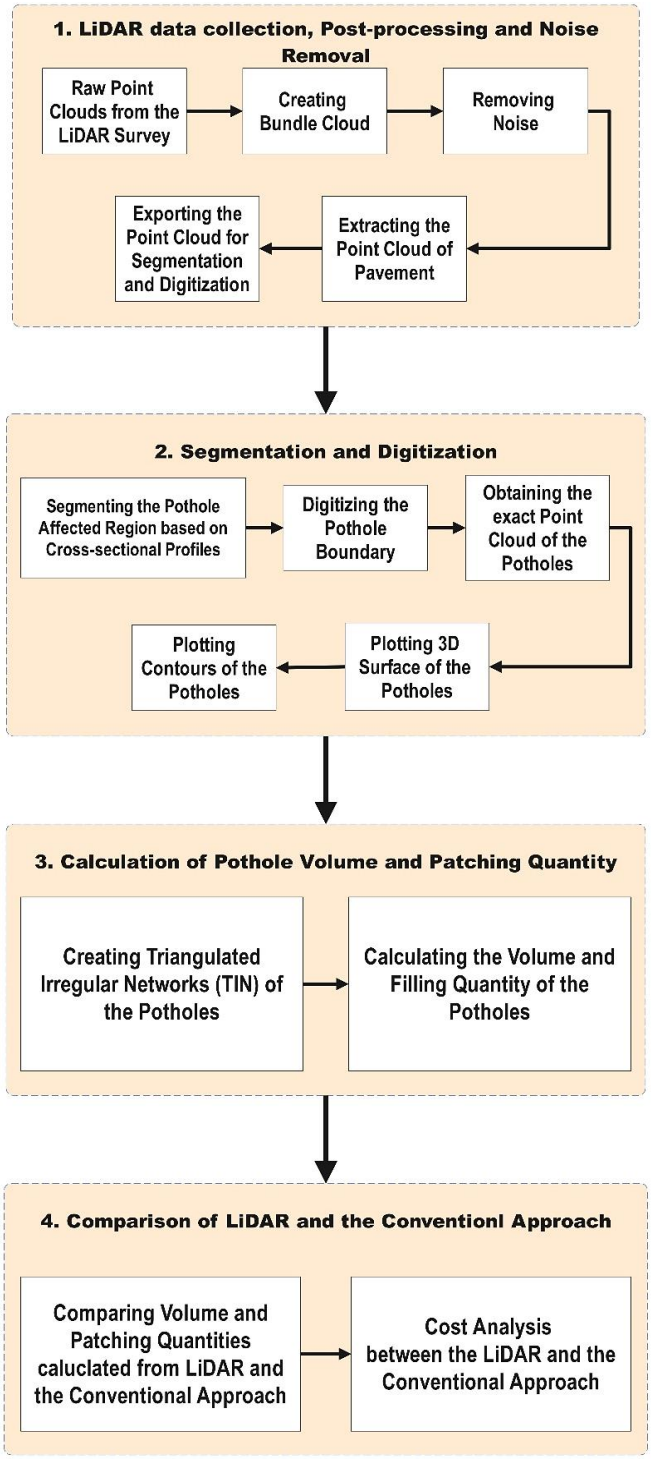

Figure 4. Flowchart showing the methodology

2.3.1. LiDAR Data Collection, Post Processing and Noise Removal

As detailed in Section 2.2, LiDAR data collection was conducted using the Leica BLK360 imaging terrestrial laser scanner for ten potholes located in and around Katpadi town in Vellore city, as illustrated in Figures 2 and 3. Adverse weather conditions—such as heavy rainfall or strong winds—can impact the effectiveness of laser scanning. Similarly, environmental factors like dense smoke or dust particles in the scanning area may interfere with data accuracy. To mitigate these issues, the scanning was carried out on a clear, sunny day with minimal traffic, ensuring that rain, lighting fluctuations, and airborne particulates would not hinder the scanning process.

In terms of surface reflectivity, pavements generally pose no significant issues, as their hard texture reflects laser beams effectively. However, wet road surfaces can absorb more laser energy, potentially leading to data gaps. Since the survey was conducted on a dry day, reflectivity concerns were minimal. Of the ten pothole locations, one scan was taken at four sites, while the remaining six locations were scanned from two different positions (see Table 1). Once the raw point cloud data were collected, the next key step in post-processing involved the creation of a bundle cloud—a process of merging individual scans using overlapping reference points to generate a single unified point cloud dataset.

Bundle cloud generation was not required at the four locations with only one scan. However, it was essential for the six potholes (labeled ‘a’ to ‘f’ in Table 1) where two scans were performed at each location. The Cyclone Register 360 software—Leica’s proprietary platform for LiDAR data processing—was used for this task.

Stitching in Cyclone Register 360 can be performed either automatically or manually. In automatic mode, the software searches for common reference points (e.g., building corners or fixed objects) during the import of raw data to automatically align and merge scans. This approach typically works well in indoor environments, where abundant fixed features aid in alignment. However, in the current study—conducted outdoors on open roadways—automatic stitching was not successful due to the limited availability of identifiable common points. As a result, manual registration was performed to align and merge the scans, as described for a representative location in the following section.

Figures 5-a and 5-b present the plan views of the raw point cloud data captured from Scan-1 (S1) and Scan-2 (S2), respectively, for Location 3, corresponding to Pothole 'c' in Table 1. These two scans were taken from opposite sides of the road by positioning the LiDAR scanner at points S1 and S2, as shown in the figures. Using Cyclone Register 360, users can not only view the plan layout but also access a full 360-degree panoramic view from each scanner position, displaying the surrounding areas captured by the LiDAR. Figures 6-a and 6-b illustrate sample 360-degree views from S1 and S2, respectively. The colors visible in Figures 5 and 6 represent the thermal data of scanned objects such as buildings, roads, and vegetation, as the LiDAR device used in this study is also equipped with a thermal imaging sensor. However, the thermal data were not utilized in this study, as the primary objective was to generate 3D models, contours, and Triangulated Irregular Networks (TINs) of the potholes using the X, Y, Z coordinate data from the point cloud, which would then be used to calculate the required patching material. From the plan views in Figures 5-a and 5-b, it is evident that common reference points—such as building corners—appear in both scans, as buildings are present on both sides of the road. These overlapping features were used to facilitate manual stitching of the scans within Cyclone Register 360, the procedure for which is detailed in the following section.

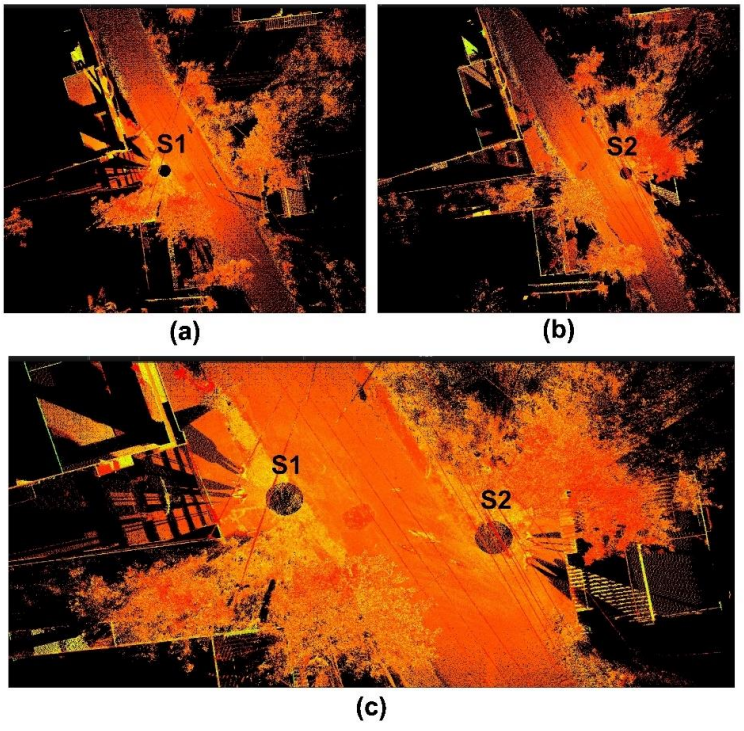

Figure 5. Plan view of the raw point cloud data from scans 1 and 2 of location 3

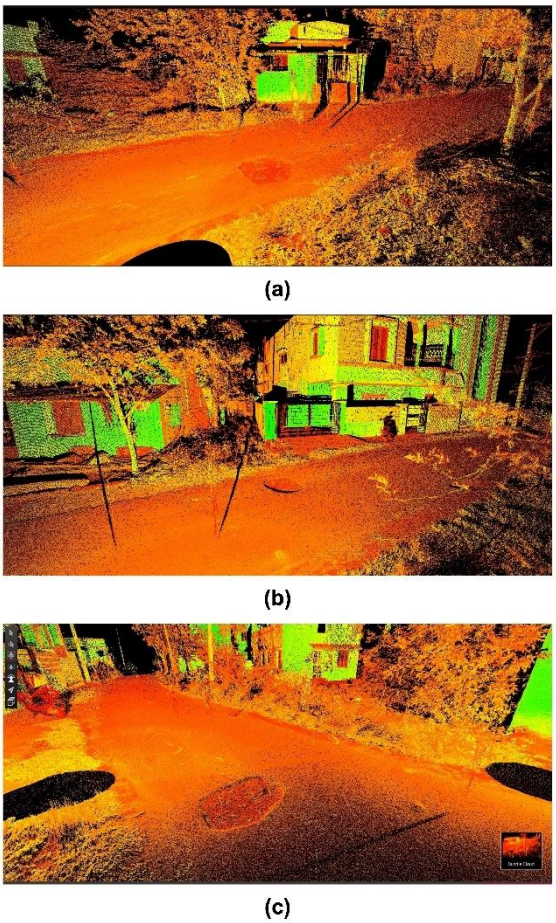

Figure 6. A sample view of the bundle cloud after stitching

Figure 7-a displays the bundle cloud for Pothole 'c' at Location 3, where the target feature—the pothole—is visible alongside other surrounding elements such as buildings, trees, and other environmental features that must be removed. This noise removal process can be efficiently performed within Cyclone Register 360 using the built-in rectangular, circular, or polygonal selection tools. The first step involves outlining the feature of interest, which in this case is the specific road segment containing the pothole.

Once the desired area is selected, the software prompts the user to choose whether to delete the data inside or outside the drawn boundary. Typically, the 'Delete Outside' option is selected, as we are interested in retaining only the pavement section that contains the pothole. By choosing this option, all elements outside the selected boundary—such as buildings and trees—are removed from the point cloud, leaving only a focused area of interest. The result of this operation is illustrated in Figure 7-b, where only the road segment with the pothole remains.

This noise removal step not only enhances the clarity and relevance of the dataset but also significantly reduces the file size. For instance, a bundle cloud composed of two scans typically occupies around 500 MB of storage (approximately 250 MB per scan). After removing the extraneous features, the refined file containing only the area of interest can be reduced to approximately 50 MB. Thus, noise removal contributes not only to data precision but also to efficient storage management.

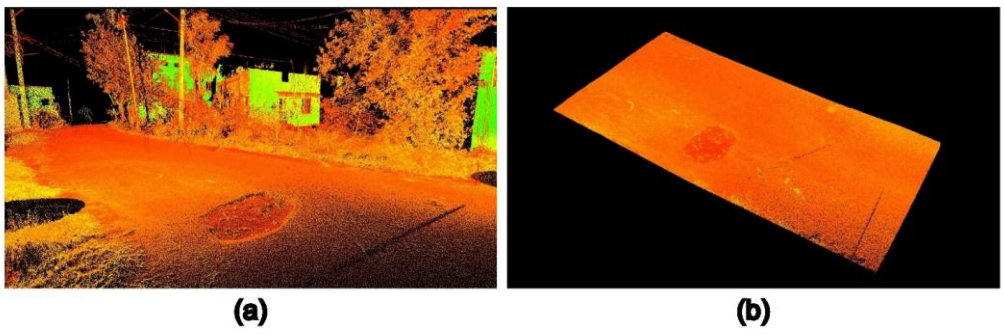

Figure 7. (a) Before noise removal (b) After noise removal

As illustrated in Figure 4, once noise removal is completed and the point cloud of the pavement containing the pothole is isolated, the next step involves exporting this refined dataset into an appropriate format for further processing, including segmentation and digitization. While several standard export formats are available—such as LAS, PTX, and PTS—the present study utilized the LAS format, as the subsequent analysis steps were performed using CloudCompare and ArcGIS, both of which require input data in LAS format. Accordingly, the cleaned bundle cloud for Pothole 'c', shown in Figure 7-b, was exported from its original BLK format to LAS format. This same procedure was followed for all other potholes in the study: after performing noise removal, the resulting point clouds were exported in LAS format to facilitate the segmentation and digitization processes, as described in the following sections.

2.3.2. Segmentation and Digitization for Generating 2D and 3D Surface of Potholes

The purpose of segmentation is to isolate the pothole-affected region from the cleaned (noise-removed) point cloud data, making it easier to subsequently digitize and extract only the pothole for further analysis. The process of segmentation and digitization is demonstrated here using the same sample pothole described earlier in Section 2.3.1—Pothole ‘c’ at Location 3.

Segmentation was performed using CloudCompare, an open-source software for processing LiDAR point cloud data. The cleaned point cloud in LAS format was imported into CloudCompare, as shown in Figure 8-a. In this visualization, red and blue colors represent differences in elevation—red indicating the highest and blue the lowest. The associated elevation scale ranges from -0.997 m to -1.223 m, with all values being negative. This is because, in terrestrial LiDAR systems, the scanner is mounted on a tripod above the ground, so any object below the scanner, such as the road and pothole surface, will naturally have negative elevation values. The total elevation difference observed was 0.226 m (22.6 cm). However, it is important to note that this value does not represent the depth of the pothole itself, since the point cloud includes both the pothole and the surrounding pavement. To isolate only the pothole, further segmentation is required, as described below.

Using the ‘Trace Polyline’ tool in CloudCompare, a polyline was drawn along the longitudinal direction of the pavement to pass through the center of the pothole (see Figure 8-a, green line). Once the longitudinal line was established, cross sections at regular intervals were generated using the ‘Extract Sections’ tool. For Pothole ‘c’, the polyline measured 7.152 meters, and the spacing between cross-sections was 0.794 meters, resulting in nine sections (labeled 1 through 9 in Figure 8-a). Across all ten potholes, polyline lengths ranged from 7.152 m to 21.783 m, and the cross-section intervals varied between 0.794 m and 2.42 m. The main objective of generating these cross-sections is to visually inspect the point cloud along each section and identify the precise location of the pothole for segmentation and digitization. Figure 8-b shows the nine extracted cross-sections, from which the presence of the pothole can be clearly identified. For example, examining these profiles reveals that the pothole is located between sections 4 and 6. Specifically, the cross-sectional graph of Section 5 shows a clear depression: the elevation decreases from left to center and then increases toward the right, indicating a typical bowl-shaped pothole profile. This observation aligns with Figure 8-a, where the pothole is visibly situated between Sections 4 and 6.

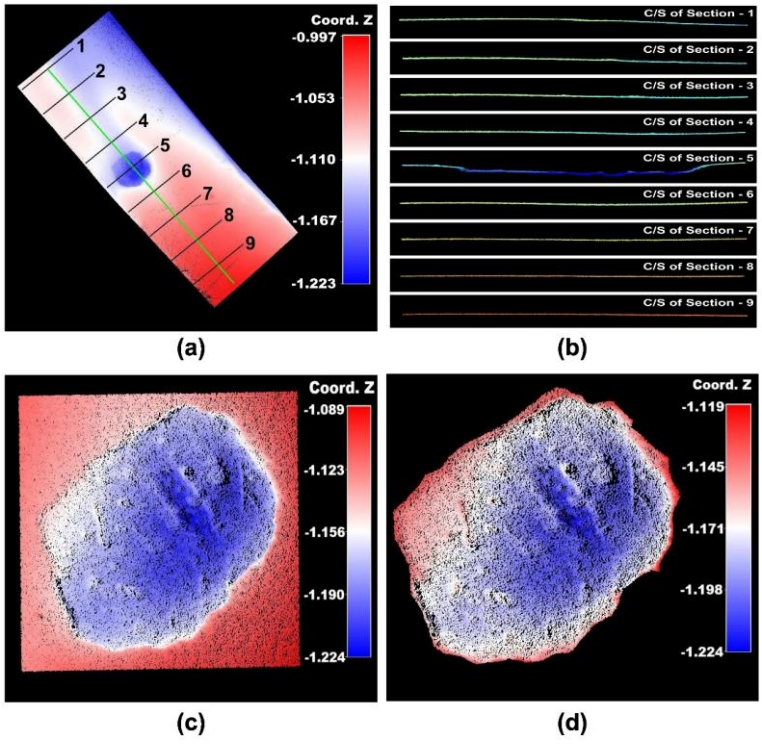

Figure 8. (a) Longitudinal and cross-sectional lines overlaid on the noise removed data (b) Extracted cross sections showing elevation changes (c) Segmented data (d) Digitized data showing only the pothole affected region

Once the exact location of the pothole was identified, the area was segmented as shown in Figure 8-c. In this figure, the elevation difference is 0.135 m (13.5 cm)—calculated as the difference between 1.224 m and 1.089 m—which is a more refined measurement compared to the 22.6 cm elevation difference observed in Figure 8-a. This improvement is attributed to the fact that Figure 8-a represents the entire pavement surface, including both the pothole and general road undulations, whereas Figure 8-c focuses solely on the pavement area surrounding the pothole. However, the rectangular segmentation shown in Figure 8-c still includes some parts of the pavement that do not contain the pothole itself. To improve accuracy, the pothole boundary was manually digitized in CloudCompare by precisely tracing its actual edges. The result of this process is presented in Figure 8-d. To ensure consistency and eliminate inter-user variability, a single operator was responsible for the entire segmentation and digitization procedure.

Following this refined digitization, the elevation difference was found to be 0.105 m (10.5 cm)—the difference between 1.224 m and 1.119 m—which represents the actual depth of the pothole. When this point cloud data, with its accurately defined boundary (Figure 8-d), is used for volume estimation and patching quantity calculations, the results are expected to be significantly more reliable and precise.

Since potholes are generally small in size, the segmentation and digitization process can typically be completed within a few minutes. However, to further reduce even this minimal time and manual effort, an automated technique was explored for detecting pothole boundaries using CloudCompare. The results of this approach are illustrated in Figure 9, using a sample pothole.

In CloudCompare, the 'SF display params' tool is used to visualize elevation ranges following segmentation (see Figure 9-b). Figures 9-a and 9-b indicate that the elevation ranges from -1.089 m to -1.224 m. The tool includes slider controls at both ends of the range bar, which can be adjusted to filter out points outside the desired elevation window. By moving the right slider to the left, non-pothole points on the pavement surface are excluded, leaving only the LiDAR points within the pothole boundary, as shown in Figures 9-c and 9-d. The adjusted elevation range is now limited to -1.148 m to -1.224 m.

This method provides an efficient alternative to manual digitization for identifying pothole boundaries. The following section explains how this segmented data is used to generate contours, 3D surfaces, and Triangulated Irregular Networks (TINs) for the purpose of calculating pothole volume and estimating the required patching quantity.

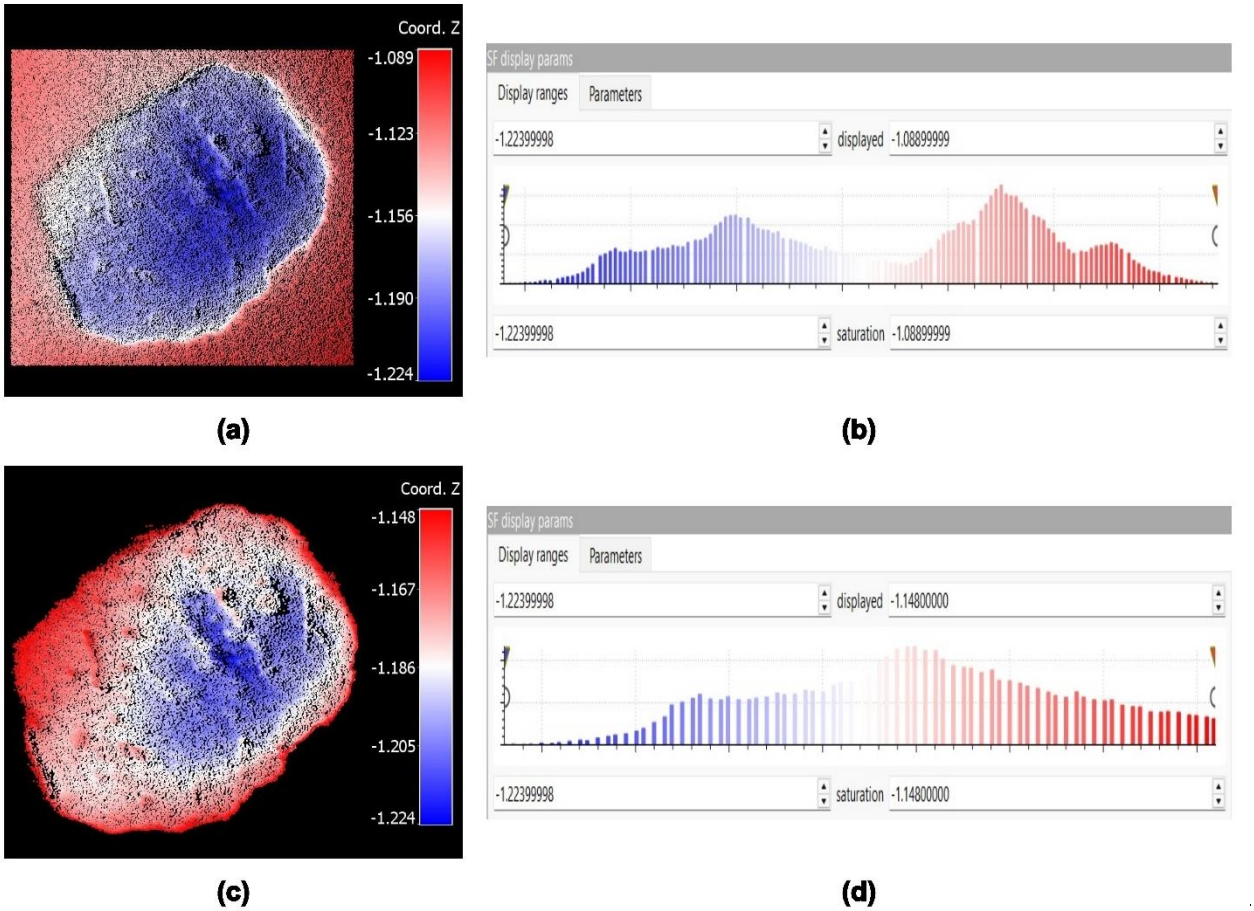

Figure 9. (a & b) Pothole and the corresponding elevation range before extraction of the pothole boundary (c & d) Pothole and the corresponding elevation range after extraction of the pothole boundary

2.3.3. Generation of 3D surface, Contours and TIN for Calculating the Pothole Volume and Patching Quantity

The segmented and digitized pothole shown in Figure 8-d was imported into OriginPro software for three-dimensional visualization and contour plotting. Although the point cloud in Figure 8-d includes elevation (Z-axis) data, its display is inherently two-dimensional. To obtain a more intuitive understanding of the pothole's geometry, the LAS file was converted to TXT format, allowing the X, Y, and Z coordinates to be imported into OriginPro for generating a 3D surface and contour map.

It should be noted that this step is optional and serves only for visualization purposes. Users may choose to skip this step and proceed directly to volume calculation, as described in the following section. To calculate the volume of a pothole, it is first necessary to generate a Triangulated Irregular Network (TIN) from the segmented and digitized point cloud (Figure 8-d). The volume estimation method used in this study is based on the TIN model, a well-established approach for representing three-dimensional surfaces using a mesh of interconnected triangles. A TIN consists of a series of adjacent, non-overlapping triangles formed from irregularly spaced data points with X, Y, Z coordinates—in this case, the LiDAR-derived point cloud of the pothole.

Each triangle in the TIN is defined by three vertices, each with known spatial coordinates. For volume calculation, this study employed the triangular prismoid method, recognized for its accuracy in computing volumes from surface data. In this method, the entire TIN is subdivided into triangular prismoids, each defined by a tilted triangle (representing the pothole surface) and a corresponding base triangle on a reference plane (which can lie above or below the prismoid). The volume of each prismoid is computed by multiplying one-third of the sum of the vertex heights by the area of the footprint triangle.

In this study, the segmented and digitized point cloud from Figure 8-d contained 42,963 points. These were used as input in the ArcGIS 10.8 3D Analyst extension, where the 'LAS Dataset to TIN' tool was applied to construct the TIN. Once the TIN was generated, the 'Surface Volume' tool in ArcGIS was used to calculate the pothole volume. An essential step in this process is defining the reference height—the horizontal plane relative to which the volume is computed. Since potholes represent depressions below the pavement surface, the volume was calculated below the reference height. The maximum elevation from the segmented data was identified and used as the reference. For example, in the case of Pothole 'c', the highest elevation was 1.119 m, which was used as the reference height to calculate the volume below this plane. Alternatively, if the lowest elevation (e.g., 1.224 m) were chosen as the reference, the volume would need to be calculated above the reference plane using the corresponding setting in the software to yield the same result. Once the pothole volume has been determined, the required patching quantity can be computed, as described in the next section.

According to Kandhal Mix [19], a 50 kg bag of cold mix asphalt is required to fill a pothole with a volume of 1.5 cubic feet. Using this guideline, the quantity of cold mix asphalt (in kilograms) was calculated for each pothole based on the accurate volume obtained from the TIN model. After determining the patching quantity for all ten potholes, the results were compared with those obtained using the conventional rectangular-based approach, in order to evaluate the potential material savings when adopting the proposed method. In the traditional method, the length, width, and depth of each pothole were used to estimate the volume, and subsequently the patching quantity, again based on the conversion rate provided by Kandhal Mix [19]. The comparative results and associated findings are presented and discussed in the following section.

3. Results and Discussion

The results of the 3D surface plots and contour maps are presented in Figure 10-a for Potholes 'a' to 'e', and in Figure 10-b for Potholes 'f' to 'h'. These visualizations provide a detailed representation of the potholes, clearly illustrating their size, shape, and both horizontal and vertical extents. The clarity and accuracy of the representations in Figure 10 can be attributed largely to the segmentation and digitization techniques employed in this study.

By isolating only the pothole-affected regions through segmentation and digitization, the resulting LiDAR point cloud contains only the data relevant to the pothole itself. This selective focus allows for the generation of precise and realistic 3D models, as shown in Figure 10.

The results also underscore the advantage of the proposed method over the conventional rectangular-based approach. While the traditional method includes both the pothole and surrounding pavement area—potentially distorting the geometry—the current approach focuses solely on the pothole boundary, enabling a more accurate and detailed 3D visualization of the actual distress. This reinforces the value of the segmentation and digitization process in improving the fidelity of pothole modeling.

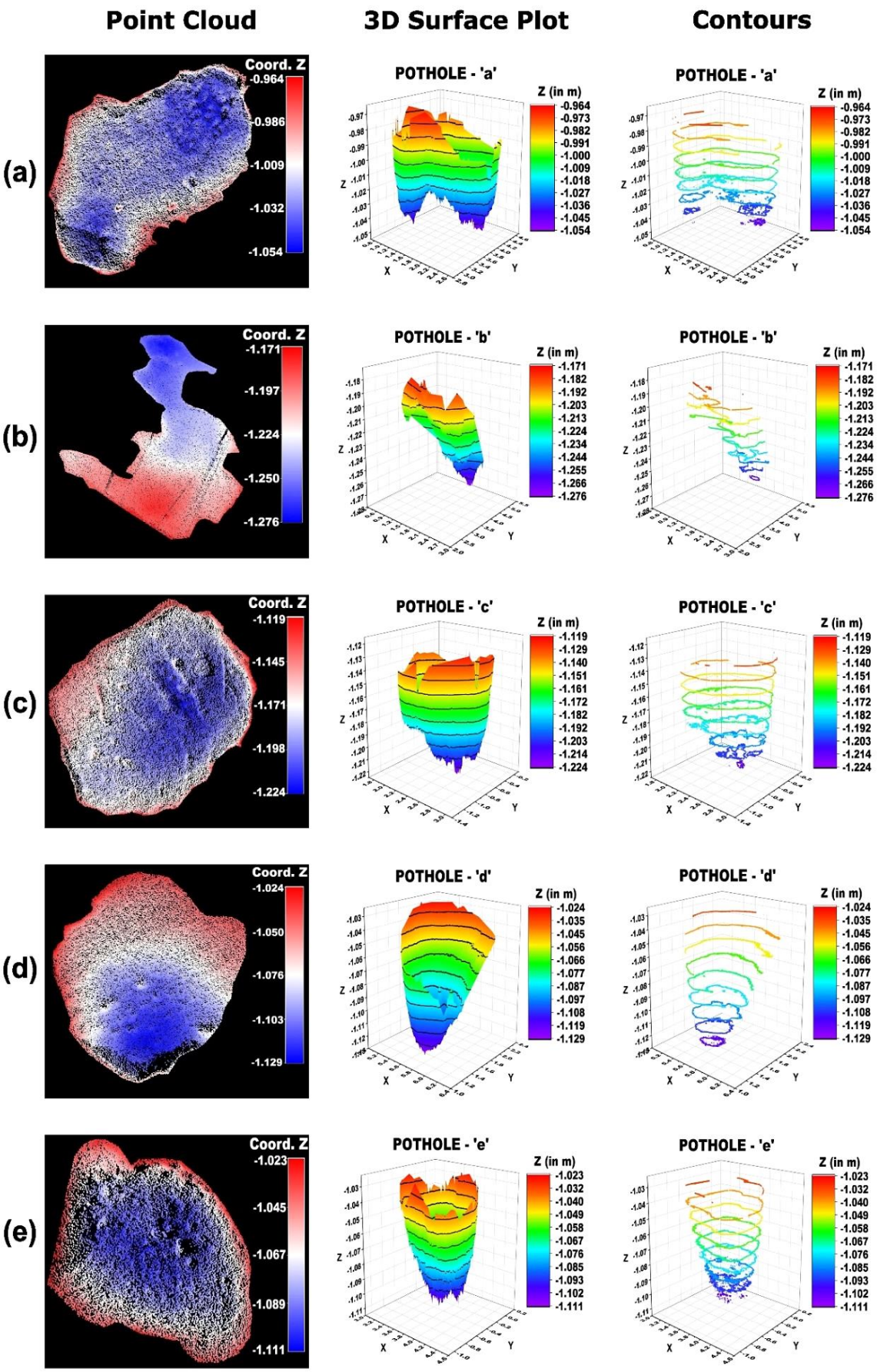

Figure 10. a) 3D Surface plot and contours for the potholes ‘a’ to ‘e’

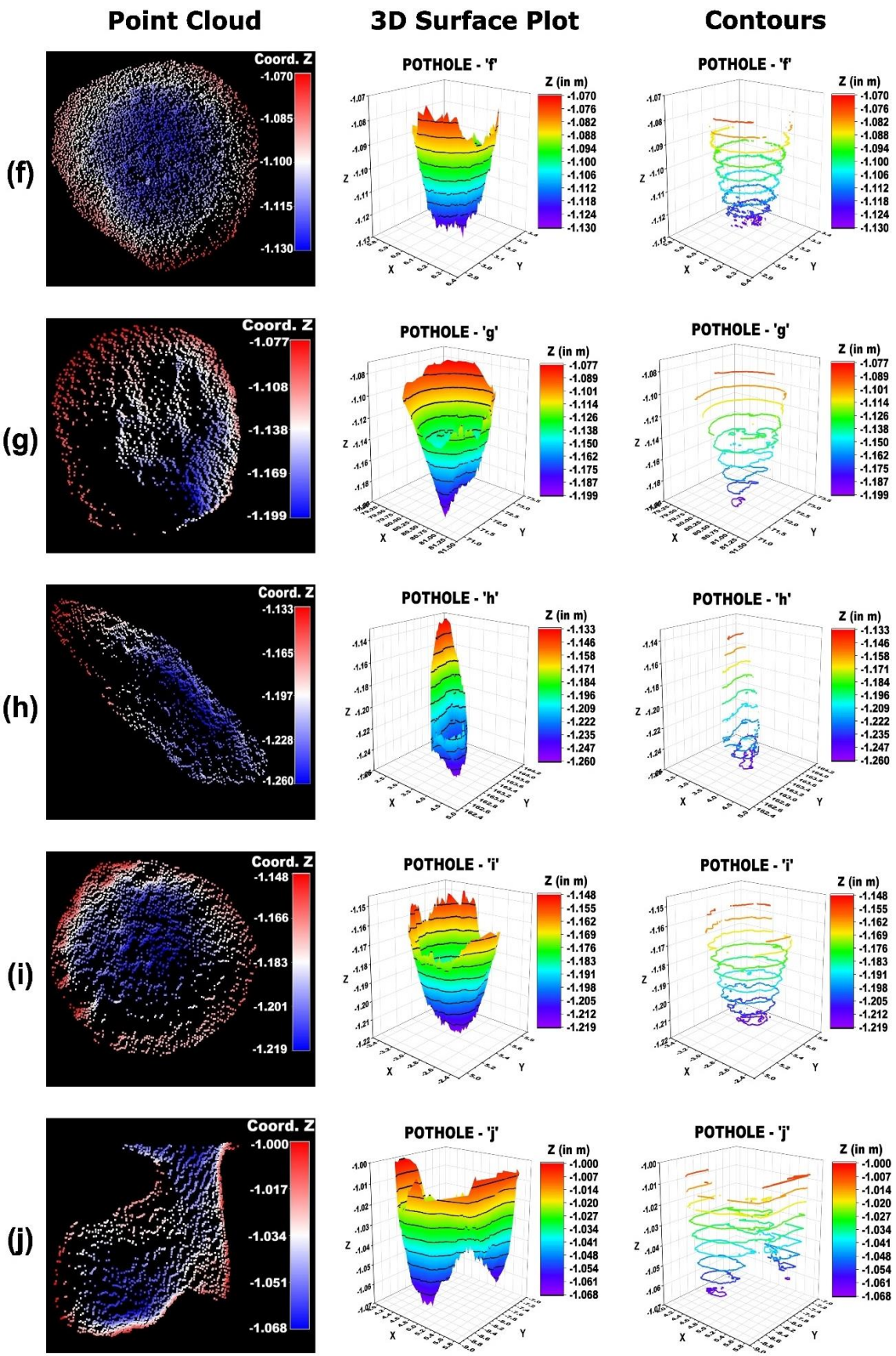

Figure 10. b) 3D Surface plot and contours of the potholes 'f' – 'j'

The 3D models of the potholes produced in this study reveal several notable insights. While it is commonly assumed that potholes are bowl-shaped depressions, the 3D visualizations in Figure 10 demonstrate that this is not always the case. Among the ten potholes analyzed, only Pothole 'e' in Figure 10-a and Pothole 'i' in Figure 10-b exhibit a classic bowl-shaped structure. The remaining potholes show variations in shape and structure.

For example, Pothole 'a' lacks a single, uniform base; instead, it presents two adjacent depressions, a feature also observed in Pothole 'j' (Figure 10-b). Pothole 'b' displays significant elevation differences within its surface—depths range from -1.276 m to -1.203 m, indicating a 7 cm variation across the pothole. Similarly, Potholes 'c' and 'd' do not exhibit uniform depth, as their profiles include multiple elevation changes, making them irregular in form. These results highlight that each pothole is structurally unique, often with notable variations in depth and shape.

The findings underscore the importance of using accurate 3D models, like those developed in this study, to reliably capture the true shape and dimensions of potholes. Such detailed models are essential not only for visual interpretation but also for precise extraction of geometric parameters such as perimeter, area, and volume, which are discussed below.

Using the 3D models and contour data shown in Figure 10, the geometric properties of all ten potholes were extracted and are presented in Table 2. According to the results, pothole perimeters range from 1.520 m to 10.774 m, with an average perimeter of 5.238 m. These results demonstrate that the terrestrial LiDAR-based segmentation and digitization approach is sensitive and accurate enough to detect even small-scale potholes, including those with a perimeter of just 1 meter.

As shown in Figure 2, Pothole 'f' is one such small pothole. Despite its size, the proposed methodology successfully captured its geometry and produced an accurate 3D model, enabling the extraction of reliable metrics. Moreover, Pothole 'f' also had the shallowest depth among all potholes evaluated, with a depth of just 0.06 m (6 cm)—the lowest recorded in Table 2. These observations reinforce the suitability of the proposed method for detecting potholes with limited dimensions in both the horizontal (X–Y) and vertical (Z) directions.

One of the key advantages of terrestrial LiDAR is its ability to capture potholes of any size, provided they lie within the scanning range. This is not always the case with Unmanned Aerial Vehicle (UAV)-based LiDAR. In terrestrial scanning, the LiDAR device is typically positioned at ground level—on the shoulder or footpath—ensuring that the entire pavement surface is covered. In many cases, a single scan can cover the full pavement width; otherwise, multiple scans can be employed to capture areas missed in the initial pass, including any distresses such as potholes.

In contrast, UAV-based surveys may miss sections of pavement due to obstructions like tree canopies. Although lowering the UAV's flying altitude can help navigate under tree cover, this comes at the cost of reduced spatial coverage and increased survey time due to the need for additional flight passes. Considering these limitations, the ground-based LiDAR approach used in this study proves to be more practical and reliable for detecting potholes of any dimension, making it highly suitable for both small- and large-scale road condition assessments.

Table 2. Geometrical Properties of the Potholes measured using Proposed and Conventional Approaches

Pothole ID (1)	Perimeter (m) (2)	Area based on digitized pothole boundary (in m^2) (3)	Length (m)(4)	Width (m) (5)	Depth (m) (6)	Area based on conventional approach (in m^2) [(4)*(5)] (7)	Ratio between the calculated areas of potholes [(7)/(3)] (8)	Volume based on TIN (in m^3) (9)	Volume based on conventional rectangular approach (in m^3) (10)	Ratio between the calculated volumes of potholes [(10)/(9)] (11)
Pothole – 'a'	5.577	1.637	1.2	2	0.09	2.400	1.466	0.092	0.216	2.348
Pothole – 'b'	10.774	2.659	2.4	2.3	0.105	5.520	2.076	0.129	0.580	4.496
Pothole – 'c'	3.505	0.818	0.9	1.15	0.105	1.035	1.265	0.050	0.109	2.180
Pothole – 'd'	3.730	0.949	1.2	1.15	0.105	1.380	1.454	0.052	0.145	2.788
Pothole – 'e'	3.915	0.961	0.95	1.3	0.088	1.235	1.285	0.048	0.109	2.271
Pothole – 'f'	1.520	0.169	0.51	0.45	0.06	0.229	1.355	0.006	0.014	2.333
Pothole – 'g'	6.957	3.422	2.1	2.25	0.122	4.672	1.365	0.190	0.576	3.032
Pothole – 'h'	6.220	1.643	0.85	2.5	0.127	2.125	1.293	0.131	0.270	2.061
Pothole – 'i'	2.905	0.602	0.9	0.96	0.071	0.864	1.435	0.024	0.061	2.542
Pothole – 'j'	7.279	1.721	1.75	1.6	0.068	2.800	1.627	0.068	0.190	2.794

Using the 3D models of potholes shown in Figure 10, surface areas were accurately calculated and are presented in Table 2. As expected, Pothole 'f' exhibited the smallest area at 0.169 m², while Pothole 'g' had the largest area at 3.422 m². These observations are also visually evident in Figure 2, where Pothole 'f' appears to have the smallest spatial footprint, and Pothole 'g' the largest. A comparison between the surface areas calculated using the proposed method and those obtained through the conventional rectangular-based approach, often used in previous studies and online calculators, yields noteworthy results. As shown in Table 2, the surface area derived from digitized pothole boundaries is consistently smaller than that obtained using the rectangular approximation for all ten potholes.

This discrepancy arises because the current study segments each pothole and digitizes its exact boundary, thereby computing area only within the true limits of the pothole. In contrast, the rectangular approach assumes that potholes are perfect rectangles, using simple length × width calculations. As a result, this method unintentionally includes portions of intact pavement surrounding the pothole, leading to overestimation of area.

These findings highlight a key advantage of the proposed approach—it not only captures the true shape and boundary of the pothole but also produces a more accurate estimation of surface area. On average, the area calculated using the rectangular approximation was found to be 1.5 times higher than that obtained through the segmentation and digitization

method. This clearly suggests that current practices relying on length and width measurements—whether in research or online tools—include non-damaged pavement, which leads to inflated results and should be avoided.

To proceed with volume calculation, it is essential to first generate a Triangulated Irregular Network (TIN). The TIN results for all ten potholes are presented in Figure 11, where gray shading indicates higher elevations and cyan shading represents lower elevations.

As with the earlier 3D models and contour plots, the TIN models also confirm that, with the exception of one or two examples, most potholes are not bowl-shaped. Each pothole is unique in shape, size, and depth. For instance, in Pothole 'a', the lowest point is -1.054 m, located at the northeastern edge (Figure 11-a), whereas in Pothole 'd', the minimum elevation is -1.129 m, occurring on the southern side (Figure 11-d). These variations are expected, as potholes are formed under different conditions and at varying stages of deterioration.

A critical observation is that the deepest point in each pothole occurs at a single location, which invalidates the assumption used in the rectangular approach—that the same depth applies uniformly across the entire pothole area. For example, in Pothole 'b', elevation gradually decreases from the south (gray) to the north (cyan), with a total depth difference of 10.5 cm (from 1.171 m to 1.276 m).

However, in rectangular volume estimation tools (e.g., online calculators as shown in Figure 12 [5–7]), this depth of 10.5 cm is applied uniformly across the entire surface area. In reality, such uniformity does not exist; depth varies continuously across the pothole surface. This discrepancy highlights a fundamental limitation of the rectangular model and further emphasizes the importance of using high-resolution 3D data—such as that generated through segmentation and LiDAR—in order to obtain accurate, spatially representative measurements for volume and patching material estimation.

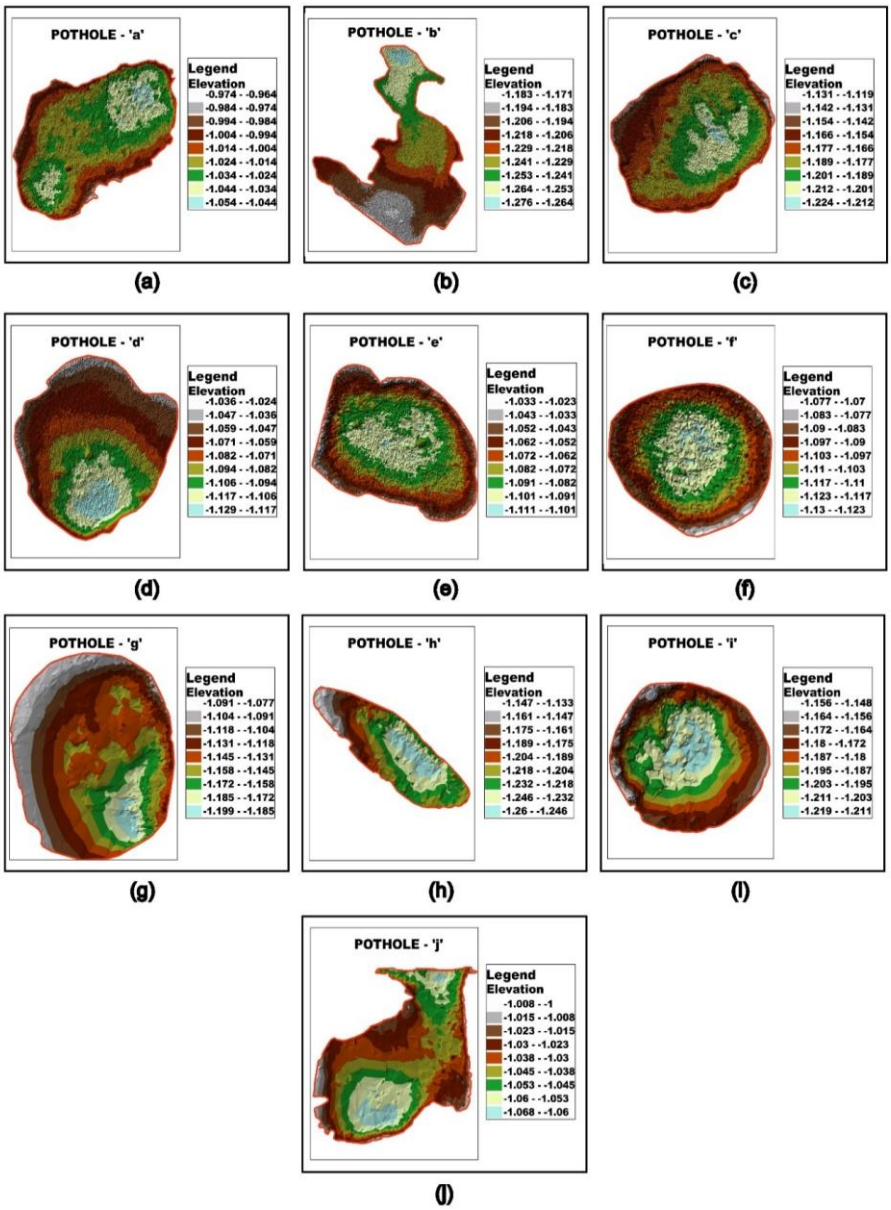

Figure 11. Triangulated irregular network (TIN) for the potholes 'a' to 'j'

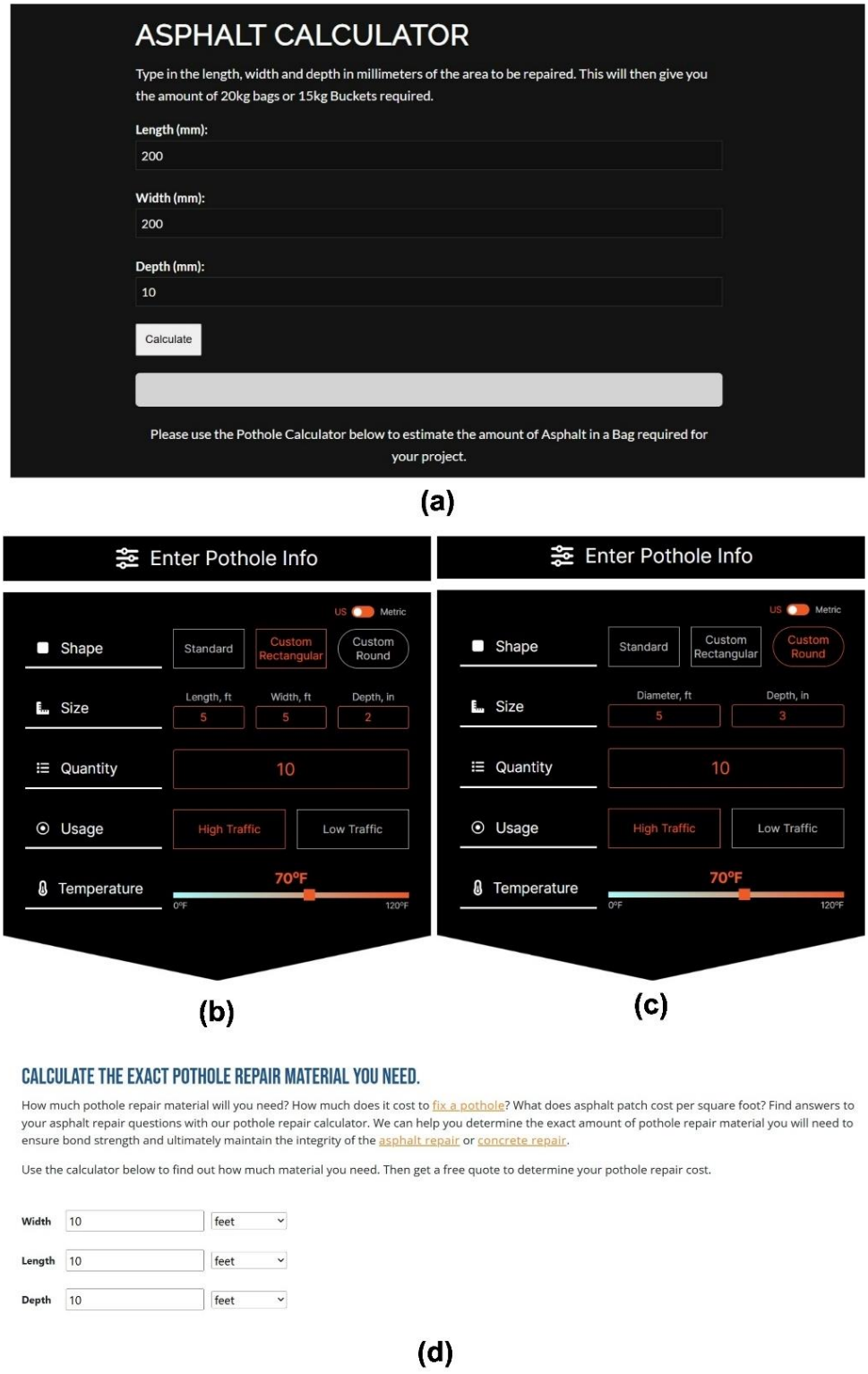

Figure 12. Online patching quantity calculators

In Figure 11, an examination of Pothole ‘f’—the smallest in the dataset—shows elevation values ranging from 1.07 m at the edges to 1.13 m at the center, resulting in a height difference of 0.06 m. This clearly demonstrates that the depth is not uniform across the pothole’s surface. Similarly, for the largest pothole, Pothole ‘g’, the elevation decreases from the northwest (gray zone in Figure 11-g) to the southeast (cyan zone in Figure 11-g), with a total difference of 0.122 m (from 1.199 m to 1.077 m). These variations are not unique to Potholes ‘f’ and ‘g’; they are evident across all ten potholes analyzed in the study. In the TIN visualizations (Figure 11), the gradient of color—from gray to cyan—indicates significant variations in depth within each pothole boundary, further confirming that depth is non-uniform. Therefore, the conventional assumption of uniform depth and cuboidal shape—as applied in previous studies and online volume calculators—is not valid. Each pothole exhibits a distinct shape, depth, and spatial structure, necessitating a more nuanced approach.

These findings clearly reveal the limitations of the rectangular approach for estimating pothole volume and patching material. The inaccuracies are not limited to depth assumptions alone. As seen in Figure 12, most online calculators also require users to input length and width, presuming that potholes are rectangular in shape. This assumption is fundamentally flawed, as evidenced by the 3D models, contours, and TIN representations in Figures 10 and 11, which show that potholes are neither rectangular nor regular in geometry.

Some calculators additionally offer a circular approximation, asking for the diameter and depth of the pothole (Figure 12-c). However, this assumption is equally problematic. The comprehensive LiDAR-based models in this study clearly demonstrate that potholes vary widely in geometry and are rarely circular. Thus, both rectangular and circular assumptions used in popular estimation tools are inaccurate. These simplified methods may lead to overestimation of the volume and, consequently, the purchase of excess patching material, resulting in unnecessary financial loss. The results of accurate volume and patching quantity calculations for all ten potholes are presented in Table 3. These values were derived from TIN models built from segmented and digitized LiDAR point cloud data, offering a highly accurate representation of each pothole's actual geometry.

In reality, it is challenging to measure pothole volume directly in the field due to their irregular shapes. However, certain geometric parameters, such as pothole depth, can be practically measured and used for validating TIN-derived data. Since depth is a critical input in volume estimation, field measurements were taken (Figure 13) and compared with TIN-based depths. The results, shown in Table 4, reveal a close correspondence between the two. The Mean Absolute Percentage Error (MAPE) was found to be only 9%, indicating strong agreement.

The low error margin can be attributed to the high registration accuracy of the point cloud during manual scan alignment, which achieved precision levels of 3–4 mm. As a result, the geometric properties derived from the TIN—constructed from the accurately registered point cloud—also reflect a comparable level of accuracy.

Figure 13. Field measurement of pothole's depth

Table 3. Patching quantity based on TIN and conventional approaches with cost saving analyses

Pothole ID	Volume based on TIN (in m^3)	Patching quantity for TIN based approach (No. of bags)	Volume based on conventional rectangular approach (in m^3)	Patching quantity for conventional approach (No. of bags)	Additional bags required if conventional rectangular approach used	Cost Savings if TIN based volume is used		
						In INR/ Pothole	In USD/ Pothole	In GBP/ Pothole
Pothole – 'a'	0.092	3.056	0.216	7.200	4.144	2901.10	219.65	125.49
Pothole – 'b'	0.129	4.285	0.580	19.320	15.035	10524.22	796.83	455.25
Pothole – 'c'	0.050	1.655	0.109	3.623	1.967	1377.09	104.27	59.57
Pothole – 'd'	0.052	1.721	0.145	4.830	3.109	2176.46	164.79	94.15
Pothole – 'e'	0.048	1.595	0.109	3.623	2.027	1419.18	107.45	61.39
Pothole – 'f'	0.006	0.195	0.014	0.459	0.264	185.13	14.02	8.01
Pothole – 'g'	0.190	6.334	0.576	19.215	12.881	9016.96	682.71	390.05
Pothole – 'h'	0.131	4.360	0.270	8.996	4.635	3244.83	245.68	140.36
Pothole – 'i'	0.024	0.813	0.061	2.045	1.231	862.00	65.27	37.29
Pothole – 'j'	0.068	2.261	0.190	6.347	4.085	2859.66	216.52	123.70
Average savings in cost						3456.66	261.72	149.53

Table 4. Comparison with ground truth measurements

Pothole ID	Depth from TIN (m)	Depth from ground observations (m)	Absolute Percentage Error (APE)
Pothole – 'a'	0.09	0.079	13.924
Pothole – 'b'	0.105	0.094	11.702
Pothole – 'c'	0.105	0.115	8.695
Pothole – 'd'	0.105	0.098	7.142
Pothole – 'e'	0.088	0.081	8.641
Pothole – 'f'	0.06	0.055	9.090
Pothole – 'g'	0.122	0.113	7.964
Pothole – 'h'	0.127	0.116	9.482
Pothole – 'i'	0.071	0.067	5.970
Pothole – 'j'	0.068	0.062	9.677
Mean Absolute Percentage Error (MAPE)			**9.229**

The volume estimated using the conventional rectangular approach relies on the pothole's length, width, and maximum depth, as illustrated in Figure 12 and detailed in Tables 2 and 3. When comparing the pothole volumes derived from the proposed TIN-based method with those obtained through the rectangular approximation, it becomes evident that the rectangular method consistently overestimates the volume—by a factor of 2 to 4.

There are two primary reasons for this discrepancy. First, the rectangular approach assumes that potholes are perfectly rectangular, leading to the inclusion of excess pavement area surrounding the actual pothole when computing surface area. Second, this method uses the maximum observed depth as a uniform value across the entire assumed rectangular footprint, effectively treating the pothole as a cuboid with constant depth, which is inaccurate.

For instance, in Pothole 'b', the minimum and maximum depths are 1.171 m and 1.276 m, respectively, yielding a depth difference of 10.5 cm. If this depth is uniformly applied over the entire rectangular area, the resulting volume becomes significantly inflated (as reflected in Table 2). This clearly illustrates the fundamental flaw in assuming uniform depth for potholes with highly variable geometry. Therefore, the rectangular model—commonly used in online calculators (Figure 12)—does not reflect the actual shape and size of potholes and may lead to over-purchasing repair material.

According to Kandhal Mix [19], one 50 kg bag of cold mix asphalt is required to fill a 1.5 cubic foot pothole. Based on this guideline, the quantity of cold mix asphalt was calculated using the volume obtained from both the TIN-based and rectangular approaches, and the results are summarized in Table 3. As anticipated, the number of bags required using the rectangular approach is 2 to 4 times higher than that calculated using the TIN-based method.

For example, for Pothole 'b', the TIN-based calculation shows that only 4 bags (50 kg each) are sufficient. In contrast, using a rectangular estimation via online tools (Figure 12), the result suggests the need for 19 bags—more than four times the actual requirement. This discrepancy significantly affects the cost of materials. At a unit cost of Rs.700 per bag [20, 21], the TIN-based estimate would require a total of Rs.2,800, whereas the rectangular method suggests a cost of Rs.13,300—an unnecessary expenditure of Rs.10,500 for just one pothole.

Table 3 outlines the cost savings for all ten potholes analyzed. On average, adopting the TIN-based method results in savings of approximately Rs.3,500 per pothole in India. These findings clearly demonstrate that the LiDAR-based segmentation and digitization approach proposed in this study is not only technically accurate but also economically advantageous. It minimizes both material waste and excess expenditure, offering a practical and cost-effective alternative to the conventional rectangular method for pothole volume estimation and patching quantity assessment.

In the United States, the average cost of a 50 lb. bag of cold mix asphalt is approximately $24 USD [22]. When converted to kilograms, this equates to roughly $53 USD for a 50 kg bag. If we assume the ten potholes analyzed in this study were located in the U.S., the cost savings per pothole achieved through the TIN-based approach are presented in Table 3. On average, this method yields a savings of $262 USD per pothole, as compared to the conventional rectangular approach.

In the United Kingdom, the average cost of a 25 kg bag of cold mix asphalt is £15.14 [23], translating to £30.28 for a 50 kg bag. Based on this rate, the average savings per pothole using the TIN-based method would be approximately £150, as shown in Table 3.

According to the Annual Road Maintenance Survey Report (2024), 2 million potholes were repaired in the UK during 2023—a 40% increase over the previous year [24]. This statistic underscores the significant annual expenditure on pothole repairs. If the LiDAR-based TIN method proposed in this study were adopted, the UK government could potentially save £300 million annually (2 million potholes × £150 per pothole).

The study utilized a Leica terrestrial laser scanner, which is priced at approximately $30,000 USD in the U.S. or £23,000 in the UK. If UK road authorities were to procure 1,000 such units, the total investment would amount to £23 million. When compared to the £300 million in potential annual savings, this one-time investment represents just one-tenth of the savings. Furthermore, as the purchase of LiDAR equipment is a non-recurring expense, the concern of high initial cost becomes negligible in light of the long-term financial benefits. These findings strongly suggest that the implementation of terrestrial LiDAR-based segmentation and TIN volume calculation, as demonstrated in this study, is not only technically effective but also economically viable. As such, it presents a cost-effective solution for national and municipal pavement management authorities aiming to optimize pothole repair expenditures.

4. Conclusion

Pavements are a fundamental component of a nation's infrastructure and play a pivotal role in the country's economy. The efficiency of transportation, including travel time between locations, is directly influenced by pavement quality. Moreover, deteriorating pavement conditions significantly impact daily life, as poor road surfaces can lead to increased vehicle operating costs and, more critically, the loss of human lives. Among the most hazardous pavement distresses are potholes, which are responsible for claiming nearly five lives per day in India—a situation similarly echoed in other countries.

In recent years, cold mix asphalt has become the preferred material for pothole repair, typically supplied in 25 kg or 50 kg bags. However, the online calculators commonly used to estimate the required patching material often assume potholes are perfect cuboids, using simple inputs like length, width, and depth to calculate volume. This assumption—of uniform surface geometry and constant depth—can result in significant overestimation, leading to excess material procurement, higher transportation costs, and unnecessary wastage.

To overcome these limitations, the present study proposes a LiDAR-based segmentation and digitization approach, utilizing only the point cloud data corresponding to the pothole itself. This data is used to generate a Triangulated Irregular Network (TIN) for accurate volume and patching quantity estimation. The methodology was validated by surveying ten potholes in Vellore, India, using a Leica BLK 360 terrestrial laser scanner. Following scan alignment and noise removal, the affected pothole regions were segmented using cross-sectional plots, and the exact pothole boundaries were digitized to isolate the relevant point cloud data.

This data was subsequently used to create 3D surface models, contours, and TINs for all ten potholes. The results demonstrated that each pothole is unique in shape, size, and depth, reinforcing the inadequacy of the conventional rectangular method, which assumes uniform geometry. The study found that the volumes and patching quantities estimated using the traditional approach were 2 to 4 times greater than those calculated using the proposed LiDAR-based TIN method. This overestimation directly translates into excessive material costs and inefficiencies in resource use.

A cost analysis further validated these findings: by adopting the proposed LiDAR-based TIN approach, one could save approximately ₹ 3,500 per pothole in India, $262 USD in the United States, and £150 in the United Kingdom. Given that millions of potholes are repaired annually in each of these countries, the implementation of this method could result in substantial national savings.

In conclusion, the use of LiDAR-derived, segmented point cloud data for volume and patching quantity estimation presents a more accurate, efficient, and economically viable alternative to the conventional rectangular approximation. This approach offers significant potential for cost savings and resource optimization in pavement maintenance operations worldwide.

5. Declarations

5.1. Author Contributions

Conceptualization, N.H.R.K. and S.V.K.; methodology, N.H.R.K. and S.V.K.; software, N.H.R.K.; validation, N.H.R.K.; formal analysis, N.H.R.K.; investigation, N.H.R.K. and S.V.K.; resources, N.H.R.K.; data curation, N.H.R.K.; writing—original draft preparation, N.H.R.K. and S.V.K.; writing—review and editing, S.V.K.; visualization, N.H.R.K.; supervision, S.V.K.; project administration, S.V.K.; funding acquisition, S.V.K. All authors have read and agreed to the published version of the manuscript.

5.2. Data Availability Statement

The data presented in this study are available on request from the corresponding author.

5.3. Funding and Acknowledgments

We would like to thank the management of Vellore Institute of Technology (VIT) for providing open access fund for publication of this article.

5.4. Conflicts of Interest

The authors declare no conflict of interest.

6. References

[1] The Economic Times. (2024). Over 2 lakh km national highways to be built by 2037, length of high-speed roads to rise 10x. The Economic Times, Mumbai, India. Available online: https://m.economictimes.com/industry/transportation/roadways/over-2-lakh-km-national-highways-to-be-built-by-2037-length-of-high-speed-roads-to-rise-10x/articleshow/108052591.cms (accessed on June 2025).

[2] Setyawan, A., Hermani, W. T., Yulianto, B., & Gravitiani, E. (2024). Influence of maintenance funds on improve road steadiness with the Curva expert program. Civil Engineering Journal, 10(2). 546-554.

[3] Isradi, M., Rifai, A. I., Prasetijo, J., Kinasih, R. K., & Setiawan, M. I. (2024). Development of Pavement Deterioration Models Using Markov Chain Process. Civil Engineering Journal, 10(9), 2954–2965. doi:10.28991/CEJ-2024-010-09-012.

[4] Ministry of Road Transport and Highways. (2022). Road Accidents in India. Ministry of Road Transport and Highways, New Delhi, India. Available online: https://morth.nic.in/sites/default/files/RA_2022_30_Oct.pdf (accessed on June 2025).

[5] Permanent Pothole Solutions. (2025). Asphalt Calculator. Permanent Pothole Solutions, Bloemfontein, South Africa. Available online: https://permanentpotholesolutions.com.au/calculator/ (accessed on June 2025).

[6] Perma-Patch. (2025). Asphalt Repair Job Calculator. Perma-Patch, Baltimore, United States. Available online: https://permapatch.com/bag-calculator/ (accessed on June 2025).

[7] Unique Paving Materials. (2025). Pothole Repair Calculator. Unique Paving Materials, Cleveland, United States. Available online: https://www.uniquepavingmaterials.com/resource-library/pothole-repair-calculator/?srsltid=AfmBOoqYbybPW8tsLSmm40SDmpXiRAeF8ul4IRhj8qyj7hlO9YxwUGl5 (accessed on June 2025).

[8] Arjapure, S., & Kalbande, D. R. (2021). Deep Learning Model for Pothole Detection and Area Computation. 2021 International Conference on Communication Information and Computing Technology (ICCICT), 1–6. doi:10.1109/iccict50803.2021.9510073.

[9] Sun, Q., Qiao, L., & Shen, Y. (2025). Pavement Potholes Quantification: A Study Based on 3D Point Cloud Analysis. IEEE Access, 13, 12945–12955. doi:10.1109/ACCESS.2025.3531766.

[10] Ravi, R., Habib, A., & Bullock, D. (2020). Pothole mapping and patching quantity estimates using lidar-based mobile mapping systems. Transportation Research Record, 2674(9), 124–134. doi:10.1177/0361198120927006.

[11] Talha, S. A., Manasreh, D., & Nazzal, M. D. (2024). The Use of Lidar and Artificial Intelligence Algorithms for Detection and Size Estimation of Potholes. Buildings, 14(4), 1078. doi:10.3390/buildings14041078.

[12] Fan, R., Ozgunalp, U., Hosking, B., Liu, M., & Pitas, I. (2020). Pothole Detection Based on Disparity Transformation and Road Surface Modeling. IEEE Transactions on Image Processing, 29, 897–908. doi:10.1109/TIP.2019.2933750.

[13] Ruseruka, C., Mwakalonge, J., Comert, G., Siuhi, S., Ngeni, F., & Anderson, Q. (2024). Augmenting roadway safety with machine learning and deep learning: Pothole detection and dimension estimation using in-vehicle technologies. Machine Learning with Applications, 16, 100547. doi:10.1016/j.mlwa.2024.100547.

[14] Park, S.-S., & Nguyen, N.-N. (2025). Two-camera vision technique for measuring pothole area and depth. Measurement, 247, 116809. doi:10.1016/j.measurement.2025.116809.

[15] Zhong, J., Kong, D., Wei, Y., & Pan, B. (2025). YOLOv8 and point cloud fusion for enhanced road pothole detection and quantification. Scientific Reports, 15(1). doi:10.1038/s41598-025-94993-0.

[16] Faisal, A., & Gargoum, S. (2025). Cost-effective LiDAR for pothole detection and quantification using a low-point-density approach. Automation in Construction, 172, 106006. doi:10.1016/j.autcon.2025.106006.

[17] Prashant Advanced Survey LLC. (2023). 3D Mobile LiDAR Survey. Prashant Advanced Survey LLC, Pune, India. Available online: https://www.prashantsurveys.com/3d-mobile-liDAR-survey.php (accessed on June 2025).

[18] Leica Geosystems. (2025). Leica Pegasus: Two Ultimate Mobile Sensor Platform. Leica Geosystems, St. Gallen, Switzerland. Available online: https://leica-geosystems.com/en-in/products/mobile-mapping-systems/capture-platforms/leica-pegasus_two-ultimate (accessed on June 2025).

[19] Kandhal Mix. (2025). An Instant All Weather Pothole Repair Solution. Madhu Agencies, Rajasthan, India. Available online: https://5.imimg.com/data5/SELLER/Doc/2022/10/CO/YT/CB/3609512/ready-mix-patch-material.pdf (accessed on June 2025).

[20] Bedrock Chem Infra LLP. (2025). Ultrabond P 8 Pothole Filling Material. Bedrock Chem Infra LLP, Village Palsai, India. Available online: https://www.bedrockcheminfra.com/ultrabond-p-8-pothole-filling-material.html (accessed on June 2025).

[21] Inam-Pro. (2017). Hincol–Roadbond. Inam-Pro, Delhi, India. Available online: https://www.india.gov.in/website-inam-pro (accessed on June 2025).

[22] Traffic Safety Warehouse. (2025). UPM Cold Mix Asphalt. Traffic Safety Warehouse, Deerfield, United States. Available online: https://www.trafficsafetywarehouse.com/UPM-Winter-Cold-Mix-2-for-Asphalt-50-Pound-Bag/productinfo/90-00018// (accessed on June 2025).

[23] Travis Perkins. (2025). Tarmac Trupack Black Cold Lay Bitumen Macadam 25kg. Travis Perkins, Northampton, United Kingdom. Available online: https://www.travisperkins.co.uk/asphalt-pothole-repair/tarmac-trupack-black-cold-lay-bitumen-macadam-25kg/p/682652 (accessed on June 2025).

[24] Asphalt Industry Alliance. (2024). Annual Local Authority Road Maintenance Survey Report 2024. Asphalt Industry Alliance, Wrington, United Kingdom. Available online: https://www.asphaltuk.org/wp-content/uploads/ALARM-survey-report-2024-FINAL.pdf (accessed on June 2025).